11

Broadband phase modulator based on a multimode channel waveguide in thin-film lithium niobate

© M.V. Parfenov, A.V. Varlamov, I.V. Ilichev, A.A. Usikova, Yu.M. Zadiranov, A.V. Tronev, P.M. Agruzov, A.V. Shamrai

Ioffe Institute, St. Petersburg, Russia
E-mail: mvparfenov@mail.ioffe.ru

Received August 1, 2024
Revised December 18, 2024
Accepted December 18, 2024

Experimental samples of integrated optical microwave modulators on thin-film lithium niobate were developed and fabricated. An approach was chosen in which optical waveguide was fabricated with larger width than required for its single-mode operation and arising high-order modes were suppressed with help of modulator electrodes placed close to the waveguide. Characteristics of the fabricated samples were measured, the correspondence between results of direct electrooptic bandwidth measurement and its theoretical estimate based on *S*-parameters measurement was demonstrated. Effective microwave modulation of optical radiation within the bandwidth of more than 30 GHz at $U_\pi L$ parameter value of $4\,\mathrm{V}\cdot\mathrm{cm}$ was demonstrated.

Keywords: lithium niobate, optical waveguides, thin-film lithium niobate, modulator, integrated optics, traveling wave electrodes.

DOI: 10.61011/TPL.2025.04.61007.20081

The use of waveguides with a high numerical aperture (i.e., strong refractive index contrast) is one of the burgeoning research trends in integrated optics [1–3]. Lithium niobate, which has proven itself well in the production of integrated optical microwave modulators [4,5], is being studied extensively as a material platform for the fabrication of thin-film lithium niobate (TFLN) waveguide modulators [1,6]. The strong refraction index contrast of TFLN waveguides allows one to reduce the transverse size of the optical waveguide mode from $\sim 10\,\mu$m [7] (a value typical of standard gradient waveguides) to $\sim 1{-}2\,\mu$m [1] at telecommunication wavelength $\lambda = 1.55\,\mu$m. Strong localization of light allows for a significant reduction of the interelectrode gap width of a modulator and, consequently, the length of traveling-wave electrodes without increase of the control voltage. In turn, the reduction in length of the electrodes decreases the requirements for matching the velocities of optical and microwave waves, thus expanding the modulation frequency band and extending the operation frequency band of TFLN-based modulators to 100 GHz and above [1].

However, one significant obstacle to the development of integrated optical devices based on high numerical aperture waveguides (specifically, TFLN-based modulators) is the stringent accuracy requirements imposed on resolution of the lithography used for their fabrication [7–9]. To ensure single-mode operation of waveguides in such devices at wavelength $\lambda = 1.55\,\mu$m, their transverse dimensions need to remain at the level $\leqslant 1\,\mu$m [10]; the resolution of standard contact photolithography used for fabrication of waveguide devices on bulk lithium niobate substrates is insufficient for such topological dimensions. In view of this, the search for an approach suitable for production of TFLN-based waveguide devices without need of a complex lithographic technology is of current concern. We have already proposed a relevant solution, which consisted in forming a waveguide with a width suitable for production by standard contact photolithography, but larger than required to achieve single-mode propagation of optical radiation. It was demonstrated [11] that such an initially multimode waveguide may be used as a quasi-single-mode one (in terms of suppression of high-order modes and unwanted intermodal interference at the waveguide output) in a modulator if its metal electrodes are positioned close to the edges of the waveguide ridge. As was found in [11], the difference in localization of intensity of optical modes in a thin film of lithium niobate (Fig. 1) makes it so that less localized high-order modes are absorbed several orders of magnitude stronger by the metal of electrodes positioned on the film, ensuring effective suppression of these modes. However, microwave modulation in such a modulator has not been demonstrated yet. The present study was aimed at investigating the applicability of the chosen approach to fabrication of an efficient integrated optical microwave modulator with a topology adapted to the resolution of standard contact photolithography.

The optical waveguide configuration and the interelectrode gap width ($5\,\mu$m) used in the low-frequency prototype were taken as a basis for microwave topology of the designed modulator [11]. The optical waveguide was fabricated based on a ridge with width $W = 2\,\mu$m formed by etching a thin ($H = 700$ nm) film of lithium niobate to depth $h = 300$ nm (Fig. 1). A dielectric buffer layer of silicon dioxide between the single-crystal lithium niobate film and

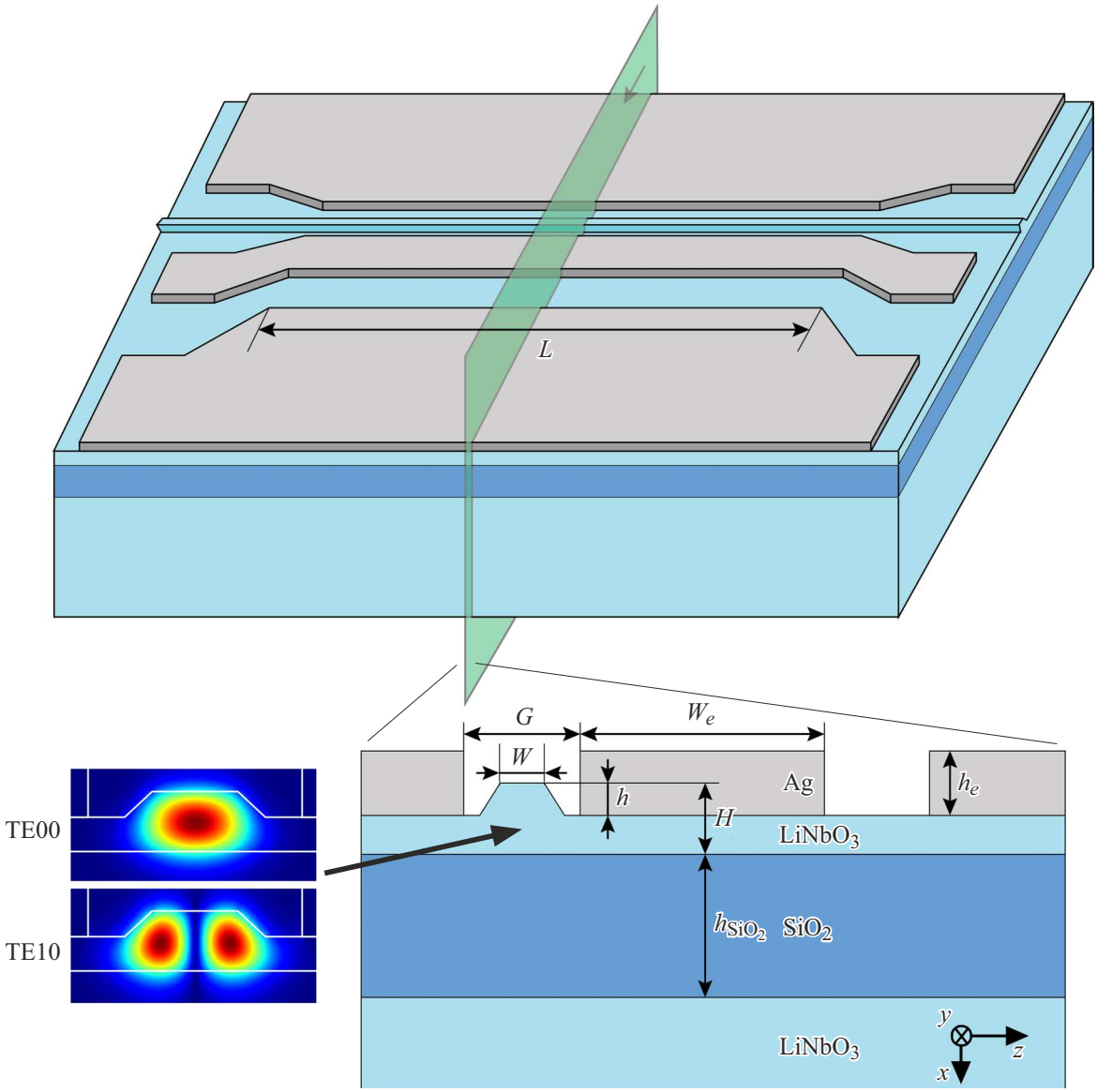

Figure 1. Microwave modulator design. The optical waveguide is formed by an etched ridge in a thin film of lithium niobate ($W = 2\,\mu$m, $h = 300$ nm, $H = 700$ nm, $h_{SiO_2} = 2\,\mu$m, $h_e = 2\,\mu$m, $G = 5\,\mu$m, $W_e = 10\,\mu$m, and $L = 10$ and 4.9 mm). The graphic insets show the distributions of the electric field magnitude of the fundamental (TE_{00}) and first higher-order (TE_{10}) modes of the optical waveguide.

the substrate with thickness $h_{SiO_2} = 2\,\mu$m, ensured a strong refractive index contrast and localization of light in the region of the etched ridge without leakage into the substrate. TFLN in the x-cut orientation (with crystallographic axis x of the single-crystal film oriented perpendicular to its surface) was used. It was assumed that the horizontally polarized TE mode of the optical waveguide, which has the most pronounced Pockels effect (the electrooptic coefficient is $r_{33} \approx 30$ pm/V) [1], would be used for modulation in this orientation. For the fabrication of the modulator the commercial thin-film lithium niobate substrate produced by NanoLN was used. The waveguides were etched using an NQII CAIBE (Intelvac) ion-beam etching system with collimated argon ions through a photoresist mask.

Microwave coplanar traveling-wave electrodes were formed along the optical waveguide (Fig. 1) to establish electrooptic modulation. They were fabricated in a galvanic process from silver and have thickness $h_e = 2\,\mu$m, interelectrode gap $G = 5\,\mu$m, and central strip width $W_e = 10\,\mu$m. Pads for interfacing the examined modulator with electrical probes were formed at the beginning and end of these coplanar electrodes in order to introduce microwave radiation.

Experimental samples of modulators of this design were fabricated in two different lengths: $L = 10$ and 4.9 mm. Electrical probes were used to measure the S parameters of electrodes, and the frequency dependences of propagation losses α and effective refraction index n_{mw} for the modulator samples of two different lengths were then extracted from

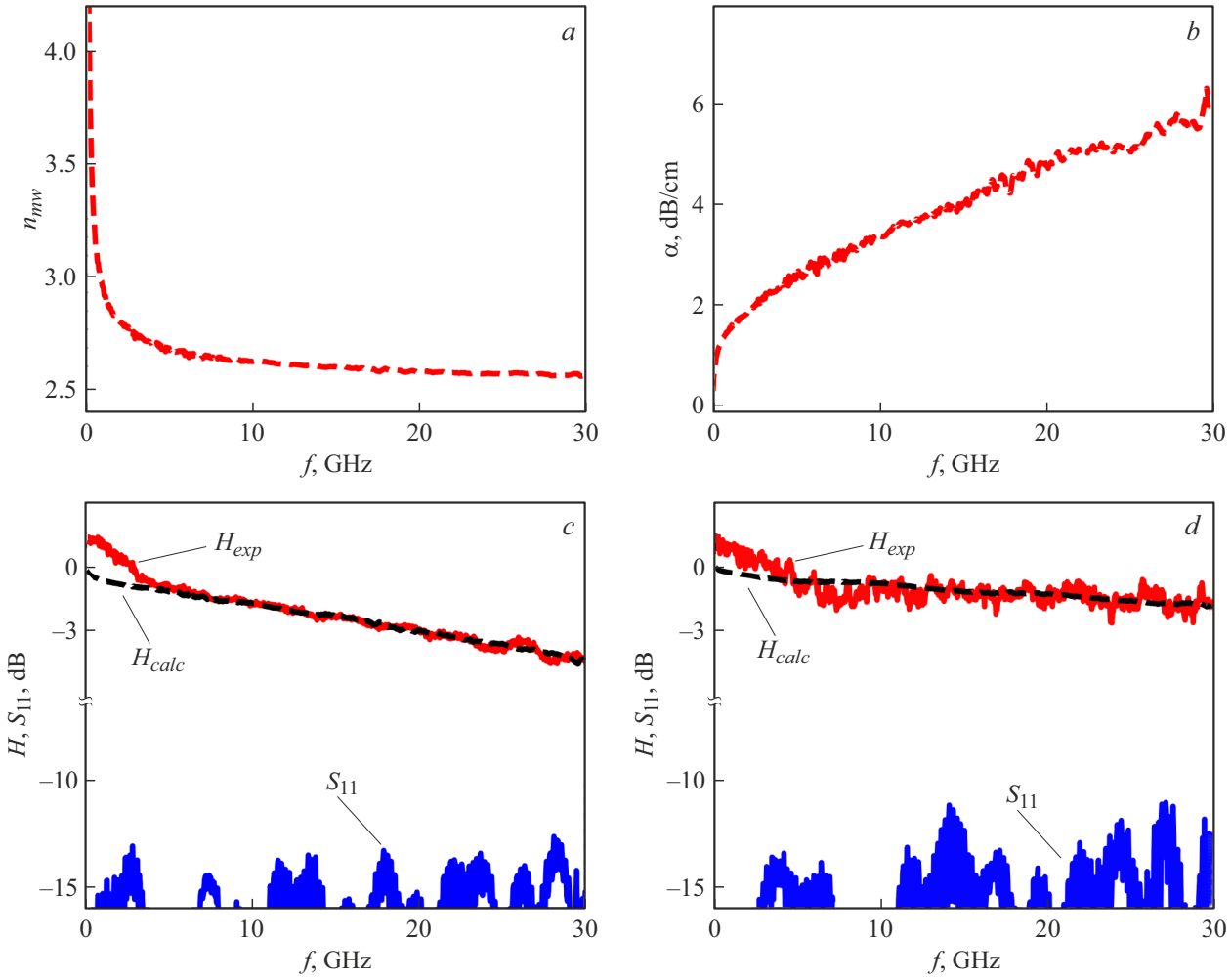

Figure 2. Frequency characteristics of the fabricated modulators. *a* — Effective microwave index n_{mw}); *b* — microwave propagation losses (α); and *c*, *d* — electrooptic response (H_{calc} — calculated based on the linear microwave parameters; H_{exp} — measured experimentally) and back reflection level (S_{11} parameter) of modulators with length $L = 10$ and 4.9 mm, respectively.

these data by matrix methods [12] (Figs. 2, *a*, *b*). These dependences were used to assess the electrooptic response of the fabricated modulators in accordance with the following well-known formula [13]:

$$H_{calc}(f) = \sqrt{(1-k(f))\frac{1-2e^{-\alpha(f)L}\cos(\xi(f)L)+e^{-2\alpha(f)L}}{(\alpha(f)L)^2+(\xi(f)L)^2}}, \quad (1)$$

where

$$\xi = \frac{2\pi f\,|n_{opt}-n_{mw}|}{c},$$

c is the speed of light in vacuum, f is the modulation frequency, α are the losses per unit length of a coplanar waveguide, L is the length of the electrooptic interaction section, k is the coefficient of reflection from the modulator input, and ξ is the parameter characterizing the propagation mismatch of microwave and optical waves with refraction indices n_{mw} and n_{opt}, respectively. It was assumed that n_{opt} is equal to the group refraction index, which was determined from the wavelength dependence of effective refraction index n_{eff}. This dependence was calculated by the finite element method near $\lambda = 1.55\,\mu$m for the fundamental waveguide mode using the formula

$$n_{opt} = \frac{c}{v_{gr}} = n_{eff} - \lambda\frac{dn_{eff}}{d\lambda},$$

where c is the speed of light and v_{gr} is the group velocity of an optical wave. Calculations were carried out with refraction indices of lithium niobate ($LiNbO_3$) ~ 2.14 and silica (SiO_2) 1.44 at wavelength $\lambda = 1.55\,\mu$m under the assumption that the angle at the base of walls of the etched ridge is 25°. The calculated group optical index value was $n_{opt} \approx 2.2$. The results of evaluation of the electrooptic response based on the obtained data are presented in Figs. 2, *c*, *d*.

After probe measurements and initial theoretical evaluation of the modulation band the fabricated samples were

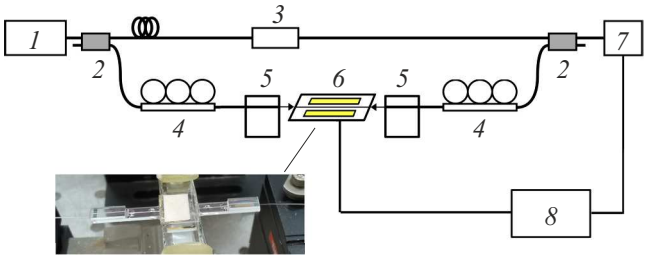

Figure 3. Diagram of the experimental setup for measuring the characteristics of the obtained modulator samples (*1* — laser, *2* — fiber splitter, *3* — attenuator, *4* — polarization controller, *5* — piezo-translation stage, *6* — modulator, *7* — photodetector, and *8* — vector network analyzer). The inset shows a photographic image of the manufactured chip coupled to optical fibers.

coupled to optical fibers. End-to-end input and output of radiation was implemented using lensed optical fibers with a modal field diameter of $2\,\mu$m. Coupling was performed with the use of specially assembled modules (substrates with cut grooves into which lensed fibers were inserted and glued). With the fibers glued in, the module substrates were glued to the end of the chips to fix the position of lensed fibers relative to the ridge optical waveguide.

The experimental setup shown in Fig. 3 was used to perform electrooptic measurements for the assembled modulator samples. This setup consisted of an interferometer with the phase modulator sample and an attenuator for optical power balancing mounted in its two arms. Since standard single mode lensed fibers were used to input (output) optical radiation into (from) the produced chips, two polarization controllers were used in the interferometer. The first one provided polarization adjustment at the input of the chip under study to ensure efficient radiation input into the TE waveguide mode, which, thank to the highest electrooptic coefficient, corresponds to the minimum control voltage in waveguide operation. The second polarization controller provided tuning to the maximum contrast of the interference pattern at the interferometer output. Electrical probes were mounted on the modulator electrodes. An R&S ZNB 40 vector network analyzer was used to measure the electrooptic microwave characteristics of the modulator. The obtained results are presented in Fig. 2 together with the calculated data. It can be seen that the nature of the electrooptic response and its slope match the calculated curves obtained earlier. The determined back reflection level is below $-10\,$dB (represented by the S_{11} parameter in Figs. 2, *c*, *d*), which is sufficient for modulator application in microwave transmission lines and corresponds to the characteristics of commercial modulators fabricated on bulk lithium niobate substrates. The product of half-wave voltage and electrode length (parameter $U_\pi L$) was measured separately at low frequencies. The obtained value is $\sim 4\,\text{V}\cdot\text{cm}$ (equivalent to $2\,\text{V}\cdot\text{cm}$ for an intensity modulator in the form of a Mach–Zehnder interferometer), which corresponds to the parameters of TFLN modulators known from literature [1].

Thus, a phase microwave modulator based on thin-film lithium niobate, which is suitable for mass production by standard contact photolithography, was designed. The possibility to provide light modulation with bandwidth in excess of 30 GHz was demonstrated experimentally. No parasitic effects associated with the conversion of optical modes, such as parasitic amplitude modulation and polarization fading, were observed in measurements. This verifies the applicability of the approach with suppression of high-order modes of an optical waveguide in fabrication of microwave TFLN-based modulators.

Conflict of interest

The authors declare that they have no conflict of interest.

References

[1] G. Chen, N. Li, J.D. Ng, H.-L. Lin, Y. Zhou, Y.H. Fu, L.Y.T. Lee, Y. Yu, A.-Q. Liu, A.J. Danner, Adv. Photon., **4** (3), 034003 (2022). DOI: 10.1117/1.AP.4.3.034003
[2] D.J. Blumenthal, R. Heideman, D. Geuzebroek, A. Leinse, C. Roeloffzen, Proc. IEEE, **106** (12), 2209 (2018). DOI: 10.1109/JPROC.2018.2861576
[3] S.Y. Siew, B. Li, F. Gao, H.Y. Zheng, W. Zhang, P. Guo, S.W. Xie, A. Song, B. Dong, L.W. Luo, C. Li, X. Luo, G.-Q. Lo, J. Lightwave Technol., **39**, 4374 (2021). DOI: 10.1109/JLT.2021.3066203
[4] E.L. Wooten, K.M. Kissa, A. Yi-Yan, E.J. Murphy, D.A. Lafaw, P.F. Hallemeier, D. Maack, D.V. Attanasio, D.J. Fritz, G.J. McBrien, D.E. Bossi, IEEE J. Sel. Top. Quantum Electron., **6** (1), 69 (2000). DOI: 10.1109/2944.826874
[5] V.M. Petrov, P.M. Agruzov, V.V. Lebedev, I.V. Il'ichev, A.V. Shamray, Phys. Usp., **64** (2), 722 (2021). DOI: 10.3367/UFNe.2020.11.038871.
[6] D. Zhu, L. Shao, M. Yu, R. Cheng, B. Desiatov, C.J. Xin, Y. Hu, J. Holzgrafe, S. Ghosh, A. Shams-Ansari, E. Puma, N. Sinclair, C. Reimer, M. Zhang, M. Lončar, Adv. Opt. Photon., **13**, 242 (2021). DOI: 10.1364/AOP.411024
[7] M.V. Parfenov, A.V. Shamrai, Tech. Phys. Lett., **46**, 819 (2020). DOI: 10.1134/S1063785020080258.
[8] K. Luke, P. Kharel, C. Reimer, L. He, M. Lončar, M. Zhang, Opt. Express, **28** (17), 24452 (2020). DOI: 10.1364/OE.401959
[9] F. Yang, X. Fang, X. Chen, L. Zhu, F. Zhang, Z. Chen, Y. Li, Chin. Opt. Lett., **20** (2), 022502 (2022). DOI: 10.3788/COL202220.022502
[10] Y. Li, T. Lan, D. Yang, Z. Wang, Results Phys., **30**, 104824 (2021). DOI: 10.1016/j.rinp.2021.104824
[11] M. Parfenov, P. Agruzov, A. Tronev, I. Ilichev, A. Usikova, Y. Zadiranov, A. Shamrai, Nanomaterials, **13** (20), 2755 (2023). DOI: 10.3390/nano13202755
[12] D. Liu, B. Gaucher, U. Pfeiffer, J. Grzyb, *Advanced, millimeter-wave technologies. Antennas, packaging and circuits* (Wiley, 2009).
[13] M. Rangaraj, T. Hosoi, M. Kondo, IEEE Photon. Technol. Lett., **4** (9), 1020 (1992). DOI: 10.1109/68.157135

Translated by D.Safin